Modeling the Impacts of Remediation Decisions on Groundwater Plume Persistence due to Back Diffusion

Eunice Yarney[1], Junqi Huang[2] and Michael C. Brooks[2]

[1]National Research Council / NAS, [2]U.S. Environmental Protection Agency/ORD/NRMRL/GWERD, Ada, Oklahoma

Eunice Yarney | yarney.eunice@epa.gov | 580-436-8838

www.epa.gov

Background

Subsurface remediation of groundwater and soils contaminated by chlorinated ethenes is a challenge as many sites remain with contaminant concentrations above regulatory limits. One issue that prevents site restoration is back diffusion of contaminants from low permeable layers into transmissive layers, which sustains contaminant plumes.

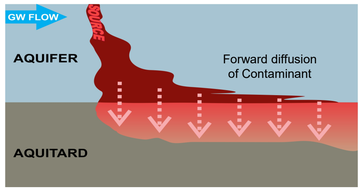

Figure 1: Forward diffusion of contaminant from aquifer to aquitard.

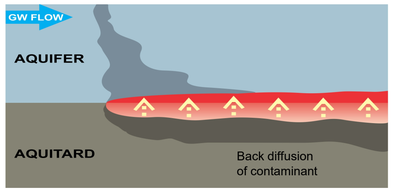

Figure 2: Back diffusion of contaminant from aquitard to aquifer.

In instances where complete remediation is impractical, modeling efforts are essential in predicting the options and expected results for partial remediation in the short term. We present results to date from a modeling framework designed to evaluate back diffusion in the context of flux-based site management. In this framework, flux and mass discharge (MD) across a down gradient control plane are evaluated as a function of back diffusion in the upgradient domain.

Research objectives

1. To investigate the sensitivity of mass discharge across a downgradient control plane (DGCP) to the mass discharge behavior from dense nonaqueous phase liquid (DNAPL) source zones and contaminant mass stored in an adjacent aquitard.
2. To explore aquitard source functions, defined as the relationship between mass discharge across the DGCP and mass stored in the upgradient aquitard.
3. To explore the benefits associated with partial removal of DNAPL mass from the source zone, as well as the impacts of when those efforts occur in the lifetime of the source zone (i.e., young versus old contaminant sites).
4. To investigate the sensitivity of mass discharge across a DGCP to contaminant spatial distribution in the aquitard and apply the power law model (PLM) to the aquitard source functions.

Methods

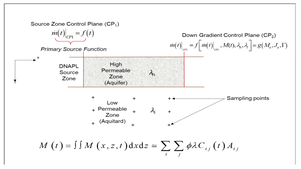

Figure 3: Graphical illustration of modeling framework.

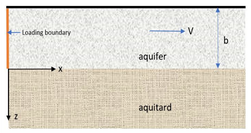

Figure 4: Model 1 - DNAPL source zone represented as a temporally-variable boundary condition.

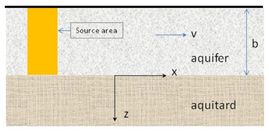

Figure 5: Model 2 - DNAPL source-zone represented as a 2D region with rate-limited dissolution from residually-saturated DNAPL.

Model 1 Equations

Governing equations for an initially clean aquifer and aquitard are:

$$R\frac{\partial C}{\partial t} = D_x\frac{\partial^2 C}{\partial x^2} - v\frac{\partial C}{\partial x} - R\lambda C - \frac{1}{\theta b}J_m,\ 0 \le x < \infty,$$

$$R_m\frac{\partial C_m}{\partial t} = D_m\frac{\partial^2 C_m}{\partial z^2} - R_m\lambda_m C_m,\ 0 \le x < \infty, 0 \le z < \infty,$$ where

$$J_m = -\theta_m D_m \frac{\partial C_m}{\partial z}\Big|_{z=0}$$

Boundary conditions:

$$C = 0,\ x \to \infty, t > 0 \quad \text{and} \quad -b_1 D_x\frac{\partial C}{\partial x} + b_2 v C = v C_0(t),\ x = 0, t > 0$$

$$C_m = C, 0 \le x < \infty, z = 0, t > 0 \quad \text{and} \quad C_m = 0, 0 \le x < \infty, z \to \infty, t > 0$$

Solutions based on Laplace transforms have been derived, but implementation is still on-going.

Model 2 Equations

Governing equations for an initially clean aquifer and aquitard are:

$$R\frac{\partial C}{\partial t} = D_x\frac{\partial^2 C}{\partial x^2} - v\frac{\partial C}{\partial x} - R\lambda C - \frac{1}{\theta b}J_m + q(x,t),\ -\infty < x < \infty,$$

$$R_m\frac{\partial C_m}{\partial t} = D_m\frac{\partial^2 C_m}{\partial z^2} - R_m\lambda_m C_m,\ -\infty < x < \infty, 0 \le z < \infty,$$ where

$$J_m = -\theta_m D_m \frac{\partial C_m}{\partial z}\Big|_{z=0} \quad \text{and} \quad q(x,t) = -\theta\rho_N\frac{\partial s_N}{\partial t}\Delta(x)$$

Boundary conditions:

$$C = 0,\ x \to \pm\infty, t > 0,\ \ C_m = 0, -\infty < x < \infty, z \to \infty, t > 0,$$

$$C_m = C, -\infty < x < \infty, z = 0, t > 0$$

Solutions based on Laplace transforms have been derived, but implementation is still on-going.

- The modeling framework is illustrated using a simplified solution presented by Tang et al. (1981). Governing equations for an initially clean aquifer and aquitard are: $\frac{R\partial C}{\partial t} = v\frac{\partial C}{\partial x} - \frac{J_m}{\theta b}$, $0 \le x < \infty$, and $\frac{R\partial C}{\partial t} = \frac{D_m \partial^2 C_m}{\partial z^2}$, $b \le z < \infty$. Boundary conditions are: $C = 0, x \to \infty, t > 0,\ C = C_0, x = 0, t > 0,\ C_m = C, 0 \le x < \infty, z = b, t > 0$; $C_m = 0, 0 \le x < \infty, z \to \infty, t > 0$

Modeling scenarios

- DGCP location scenarios: L=10 (L10) and 500 (L500) m away from the primary source zone control plane (SZCP).
- Scenario 1: No remediation (NR).
- Scenario 2: Young site with 100% remediation (Y100). A young site is defined as one where 80% of contaminant remains as DNAPL and 20% is in the plume.
- Scenario 3: Old site with 100% remediation (O100). An old site is the opposite of the young site, where 20% of contaminant remains as DNAPL and 80% is in the plume.
- For sensitivity of mass discharge to contaminant spatial distribution analysis: NR_L10 scenarios for initial contaminant concentrations (C0) = 100 and 1000 mg/l.

Results

A. Mass in the Aquitard as a Function of Time

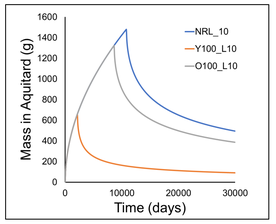

Figure A1: Mass in domain between DGCP and SZCP for L10.

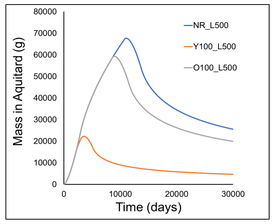

Figure A2: Mass in domain between DGCP and SZCP for L500.

Figures A1 and A2

- Results for both L10 and L500 show that early remediation curtails forward diffusion of contaminant, thus peak mass is smallest for Y100, followed O100 and NR. Peak mass for L10 = {600, 1300, 1400} g, and for L500 = {22000, 59000, 67000} g for cases Y100, O100 and NR respectively.
- Peak mass for L500 is greater than that for L10 by a factor of 37, 45 and 48 for cases Y100, O100 and NR respectively.

B. Primary and Secondary Source Strength Functions (SSFp & SSFs)

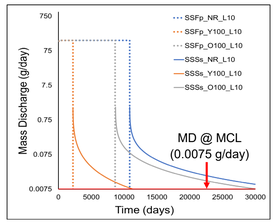

Figure B1: SSFp and SSFs for L10.

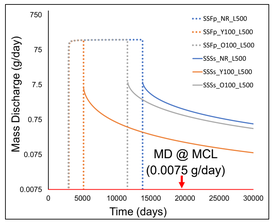

Figure B2:SSFp and SSFs L500.

Figures B1 and B2

- Results for both L10 and L500 show that maximum (max) MD due to back diffusion from secondary source is relatively insensitive to the timing of remediation: maxMD for L10 = {1.8, 1.7, 1.8} g/day and for L500 = {9.0, 6.2, 8.6} g/day, for cases NR, Y100, and O100, respectively.
- MaxMD due to back diffusion at L10 is smaller than that of L500 by a factor of 5 for cases NR and O100, and by a factor of 4 for case Y100.
- Timing of remediation does impact the longevity of risk. Time to reach a MD (0.0075) g/day that reflects an MCL of 0.005 mg/L = {31, 83, 98} years for L10, and {390, 970, 1100} years for L500 for cases Y100, O100, and NR respectively.
- Time to reach a MD that reflects MCLs at L500 is about an order of magnitude larger for all three cases, compared to L10.

C. Aquitard Source Functions (AQSF)

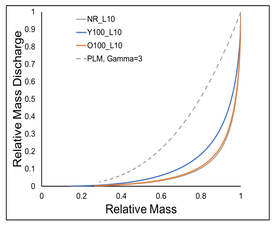

Figure C1: AQSF for L10.

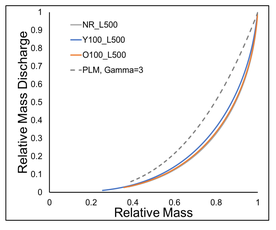

Figure C2: AQSF for L500.

Figures C1 and C2

- AQSF for L10 has greater initial decline in MD as relative mass decreases, but then more tailing compared to the AQSF for L500.
- AQSF for L500 has a more uniform change in relative MD as relative mass decreases, compared with AQSF for L10.
- AQSF are less sensitive to timing of remediation for L500, compared to L10.
- PLM with Gamma = 3 is included for comparison.

$$\frac{MD}{MD_{\max}} = \left(\frac{M}{M_{\max}}\right)^{\Gamma}$$

Where M = Mass in aquitard, Γ = Gamma.

D. How does an AQSF based on the 1D model compare with the 2D model?

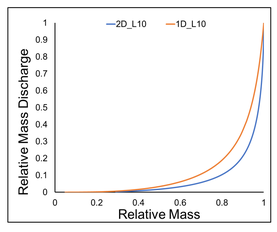

Figure D1: AQSF for L10 using 1D and 2D models.

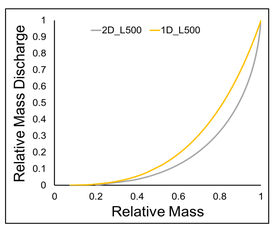

Figure D2: AQSF for L500 using 1D and 2D models.

Figures D1 and D2

- The 1D model matches the 2D model qualitatively, with both models reflecting the extensive tailing behavior associated with back diffusional transport (i.e., large reductions in relative MD as relative mass initially decreases, followed by increasingly smaller reductions in relative mass discharge as relative mass decreases).
- In both cases, the 2D model results in greater MD reduction as mass decreases at early time (i.e., upper right corner), but more tailing is predicted at late time (i.e., lower left corner).
- E.g., for L10, a 20% reduction in mass (80% relative mass remaining) results in an 80% reduction in relative flux based on the 1D model, but a 90% reduction based on the 2D model. For L500, a 20% reduction in mass results in a 50% reduction in relative MD for the 1D model, but a 70% reduction in relative MD based on the 2D model.

Results cont'd

E. Is Mass Discharge Across a DGCP Sensitive to Contaminant Spatial Distribution in the Aquitard?

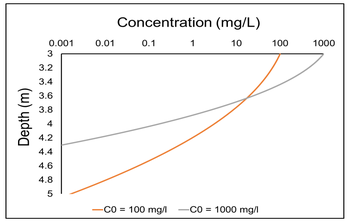

Figure E1: Contaminant spatial distribution in aquitard for C0 = {100, 1000} mg/L.

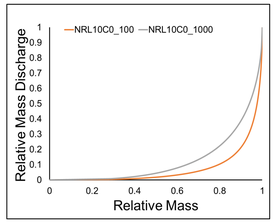

Figure E2: AQSF for L10. C0 = {100, 1000} mg/L.

Figures E1 and E2

- To explore this question, AQSF were generated for C0 = {100, 1000} mg/L, but the longevity of the primary source in each case was adjusted such that the maximum mass in the aquitard was identical.
- Figure E1 shows the spatial concentration distribution at 5 m downgradient from the SZCP at the time of maximum aquitard mass for the two cases, and illustrates the difference in spatial distribution.
- Figure E2 shows the AQSF for the two cases, and illustrates that while the AQSFs are qualitatively similar, they are quantitively different.
- Both AQSF display characteristics of diffusional tailing (i.e., large reductions in relative MD as relative mass initially decreases, followed by increasingly smaller reductions in relative MD as relative mass decreases). However, the case of C0 = 100 mg/L has greater tailing characteristics relative to the case of C0 = 1000 mg/L. This indicates that MD across a DGCP is sensitive to the spatial distribution of contaminant in the aquitard.

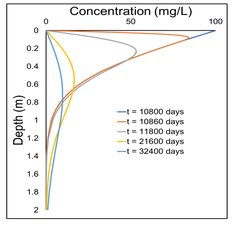

Figure E3: Contaminant spatial distribution in aquitard after complete dissolution of primary contaminant (t >= 10860 days).

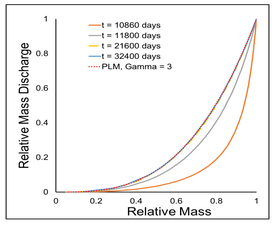

Figure E4: AQSF after complete dissolution of primary contaminant (t >= 10860 days).

Figures E3 and E4

To further explore this question, AQSF were generated using a one-dimensional (1D) diffusion model.

- Figure E3 illustrates contaminant spatial distributions. For the AQSF shown in Figure E4, the relative mass and MD were based on the mass in and MD from the aquitard at t = {10860, 11800, 21600, 32400} days.
- Results show that with increasing time, AQSF converge to the PLM with Gamma = 3.
- This may be advantageous for predicting back diffusion behavior at relatively old sites.

Conclusions

Simplified equations were used to illustrate the evaluation of back diffusion in a flux-based site management framework. Future work will implement more complex models using more realistic representations of the primary DNAPL source zone. Preliminary conclusions from work completed to date are as follows:

1. MD across a DGCP is sensitive to contaminant mass stored in an adjacent aquitard. DGCP locations closer to the primary SZCP had smaller maximum MD due to back diffusion, compared to locations further away from the SZCP.
2. As expected, the timing of remediation does impact the longevity of risk at contaminated sites.
   a. Early remediation reduced the amount of mass in the aquitard from forward diffusion and subsequently, plume persistence due to back diffusion.
   b. Compared to later remediation, early remediation resulted in sites achieving MCLs at a DGCP in a relatively shorter time. However, the calculated maximum mass discharge due to back diffusion was insensitive to the timing of remediation.
3. AQSF are less sensitive to the timing of remediation as the distance from the SZCP increases. Also, AQSF at DGCPs further away from the SZCP appear to display less diffusive tailing behavior relative to DGCPs located closer to the SZCP.
4. MD across a DGCP is sensitive to spatial distribution of contaminant in the aquitard and with increasing time, AQSF converge to the PLM with Gamma = 3. This may be advantageous for predicting back diffusion behavior at relatively old sites
5. AQSF based on 1D and 2D models compared well by reflecting the extensive tailing behavior associated with back diffusional transport. However, the 2D model predicted 10% and 20% more MD reduction for same decrease in mass closer and further away from the SZCP respectively.

Disclaimer and Acknowledgements: The views expressed in this poster are those of the authors and do not necessarily represent the views or policies of the U.S. Environmental Protection Agency. We thank Srijan Dhakal for his support with modeling work and Kathy Tynsky for her support in poster preparation.